Molecular cloning and characterization of six novel isoforms of human Bim, a member of the proapoptotic Bcl-2 family[1]

Mami U, Toshiyuki Miyashita*, Yoshiaki Shikama, Keiko Tadokoro, Masao Yamada

Department of Genetics, National Children's Medical Research Center, 3-35-31 Taishido, Setagayaku, Tokyo 154-8509, Japan

Received 10 October 2001; accepted 31 October 2001

First published online 16 November 2001

Edited by Vladimir Skulachev

Abstract Bim protein is one of the BH3-only proteins, members of the Bcl-2 family that have only one of the Bcl-2 homology regions, BH3. BH3-only proteins are essential initiators of apoptotic cell death. Thus far, three isoforms of Bim have been reported, i.e. Bim_{EL}, Bim_L and Bim_S. Here we report the cloning and characterization of six novel isoforms of human Bim, designated as Bimα1, α2, and β1–β4, which are generated by alternative splicing. Unlike the three known isoforms, none of these novel isoforms contained a C-terminal hydrophobic region. Among the novel isoforms, only Bimα1 and α2 contained a BH3 domain and were proapoptotic, although less potent than the classical isoforms. These two isoforms localized, at least in part, in mitochondria when transiently expressed in HeLa cells as a green fluorescent protein-fused form. These results suggest that the BH3 domain is necessary for induction of apoptosis and mitochondrial localization but not sufficient for the full proapoptotic activity. While the classical isoforms were always predominantly expressed in transformed cells, expression profiles of *bim* isoforms were highly variable among normal tissues at least in humans, suggesting a tissue-specific transcriptional regulation of *bim*.

Key words: Apoptosis; Mitochondrion; Bim; Alternative splicing

1. Introduction

Apoptosis or programmed cell death is a physiologic process that is regulated by evolutionarily conserved genes. Cells undergoing apoptosis exhibit certain morphological and biochemical characteristics such as cell shrinkage, plasma membrane blebbing, chromatin condensation and DNA fragmentation. Apoptosis is critical for the development and the maintenance of all metazoans. Thus, dysregulation of apoptosis can contribute to many major diseases including cancer, autoimmune disorders and certain neurodegenerative diseases [1]. Apoptotic signals are mainly transduced through two relatively distinct pathways: the so-called 'intrinsic' pathway mediated by mitochondria from which proapoptotic molecules such as cytochrome *c* are released into the cytosol and an 'extrinsic' pathway triggered by members of the tumor necrosis factor (TNF) receptor superfamily such as Fas (Apo-1/CD95) or TNF-α receptor [2].

One of the major components of cell death machinery is the Bcl-2 family. To date, at least 20 members of this family have been reported in mammals. Bcl-2 family proteins either reside constitutively on the mitochondrial membrane or translocate to mitochondria in response to apoptotic stimuli and regulate the release of proapoptotic molecules from mitochondria. Thus they work as important sensors for cell death signals [3]. Despite structural similarity, members of the Bcl-2 protein family have either an anti-apoptotic or proapoptotic function. The proapoptotic Bcl-2 subfamily is further divided into two groups. One includes 'multi-domain' or 'Bax-like' proteins that have three Bcl-2 homology domains (BH1–3) and the other includes 'BH3-only' proteins that share sequence homology only within the BH3 domain [4]. At least nine mammalian BH3-only family members (Bad, Bik, Blk, Hrk, Bid, Bim, Noxa, PUMA, Bmf) have been identified. Bim was initially isolated by screening a cDNA expression library with a Bcl-2 protein probe [5]. Three Bim isoforms have been reported and designated as Bim_{EL}, Bim_L and Bim_S, all of which bind to Bcl-2 and induce apoptosis, Bim_S being the most potent. The biological importance of these molecules is underscored by the analysis of *Bim*-deficient mice in which lymphoid, myeloid and plasma cells accumulate and autoimmune kidney disease is developed due to impaired apoptosis [6]. Furthermore, Bim was recently reported to play an important role in neuronal and hematopoietic cell death caused by trophic factor deprivation [7–9].

Here we describe novel isoforms of human Bim and discuss their functions, subcellular localizations and expression profiles.

2. Materials and methods

2.1. Isolation and expression plasmid construction of human Bim isoforms

Polyadenylated RNAs from human tissues (Clontech) were reverse-transcribed and cDNAs encoding Bim were amplified by the polymerase chain reaction (PCR) using SuperScript One-Step reverse transcription-PCR (RT-PCR) with Platinum *Taq* (Life Technologies, Inc.) according to the manufacturer's protocol. The primers used

*Corresponding author. Fax: (81)-3-3414 3208.
E-mail address: tmiyashita@nch.go.jp (T. Miyashita).

[1] The cDNA sequences of Bimα1, Bimα2, Bimβ1, Bimβ2, Bimβ3 and Bimβ4 have been deposited in GenBank under accession numbers AB071195–AB071200.

Abbreviations: BH, Bcl-2 homology; $\Delta\Psi_m$, mitochondrial membrane potential; EGFP, enhanced green fluorescent protein; GAPDH, glyceraldehyde-3-phosphate dehydrogenase; PCR, polymerase chain reaction; RT-PCR, reverse transcription-PCR; TNF, tumor necrosis factor; zVAD-fmk, carbobenzoxy-VAD-fluoromethyl ketone

0014-5793/01/$20.00
PII: S0014-5793(01)03145-3

for the amplification were 5′-GGAATTCATGGCAAAGCAACC-TTCTGA-3′ and 5′-GCGTCGACTCAATGCATTCTCCACACC-3′ (*Eco*RI and *Sal*I linker sequences are underlined). The amplified products were digested with *Eco*RI and *Sal*I, gel-purified and subcloned into pEGFP-C2 (Clontech). For the amplification of *bid* cDNA, the primers 5′-CCATGGACTGTGAGGTCAAC-3′ and 5′-GTCCATC-CCATTTCTGGCTA-3′ were used.

2.2. Cell cultures and transfections

The human embryonic kidney cell line 293 and human cervical cancer cell line HeLa were maintained in Dulbecco's modified Eagle's medium supplemented with 10% fetal calf serum, 100 U/ml penicillin and 0.1 mg/ml streptomycin at 37°C in a humidified atmosphere of 5% CO_2. Cells were transfected with the plasmids described above using Effectene reagent (Qiagen) according to the manufacturer's protocol. Carbobenzoxy-VAD-fluoromethyl ketone (zVAD-fmk) (Peptide Institute, Osaka, Japan) was added in some experiments to a final concentration of 50 μM.

2.3. Confocal microscopy

At 24 h posttransfection, the cells growing on glass-bottomed culture dishes were stained with 250 nM of MitoTracker Red (Molecular Probes) and fluorescent images were obtained using a confocal microscope (Fluoview FV300, Olympus, Tokyo, Japan).

2.4. Immunoblotting

Immunoblot analysis was performed as described previously [10]. In brief, 30 μg of the cell lysate was subjected to SDS–PAGE and transferred onto a nitrocellulose membrane. The membrane was incubated with rabbit anti-green fluorescent protein (GFP) polyclonal antibody (MBL, Nagoya, Japan) followed by horseradish peroxidase-conjugated anti-rabbit immunoglobulins (Sigma). The proteins were visualized by using enhanced chemiluminescence immunoblotting detection reagents (Amersham).

2.5. Luciferase assay

293 cells growing on six-well culture plates were cotransfected using Effectene reagent with various combinations of the expression plasmids encoding isoforms of Bim fused with enhanced green fluorescent protein (EGFP) and pGV-C2 (Wako Chemicals, Osaka, Japan) that encodes luciferase. After 48 h, the cells were washed once with phosphate-buffered saline to remove dead and floating cells. They were then harvested and subjected to luciferase assay as described previously [11].

2.6. Analysis of bim isoform expression profiles

Human *bim* cDNA was amplified by RT-PCR as described using total RNA purified from a panel of cell lines and human tissues (Ambion and Clontech). 1 μl of logarithmically amplifying PCR product was applied onto a DNA LabChip (Agilent Technologies) and loaded into an Agilent 2100 bioanalyzer according to the manufacturer's protocol. Data analysis was performed with Agilent 2100 bioanalyzer software.

2.7. Real-time quantitative RT-PCR

To quantify the transcript of *bim*, *bim* cDNA was amplified by RT-PCR using the reagents described above and primers 5′-TGATGT-AAGTTCTGAGTGTG-3′ and 5′-ACGTAACAGTCGTAAGATA-A-3′. One-step RT-PCR was performed using a 7700 ABI PRISM Sequence Detector System (Perkin Elmer-Applied Biosystems). To normalize the expression of *bim*, the glyceraldehyde-3-phosphate dehydrogenase (*GAPDH*) housekeeping gene was also amplified, using primers 5′-GAAGGTGAAGGTCGGAGT-3′ and 5′-GAAGATGG-TGATGGGATTTC-3′. Fluorogenic probes 5′-ACCTCCCTACAG-ACAGAGCC-3′ and 5′-CAAGCTTCCCGTTCTCAGCC-3′ carrying 5′ 6-carboxy-fluorescein as a reporter dye and 3′ 6-carboxy-tetramethyl-rhodamine as a quencher dye were used to detect the PCR product of *bim* and *GAPDH*, respectively. In every experiment, *GAPDH* was amplified using a series of dilutions of a known amount of the standard RNA supplied by Perkin Elmer to prepare a standard curve. Data analysis was performed as described [12] with slight modification.

3. Results

3.1. Isolation of novel isoforms of human bim

In the course of obtaining cDNA for the entire coding region of human Bim using RT-PCR, we observed multiple amplified products, whereas a single product was obtained for human cDNA encoding Bid, for which no isoforms have been reported (Fig. 1A). This prompted us to sequence each product to see if they contained novel isoforms. As a result, in addition to the three known isoforms of *bim* (EL, L and S), we have cloned six novel isoforms and designated them bimα1, α2, and β1–β4 (Fig. 1B). Using the genome sequence of *bim* provided by Celera Genomics, three unidentified exons were discovered in the *bim* locus and all isoforms were confirmed to be produced by alternative splicing (Fig. 1C). Among the novel isoforms, *bim*α1, α2, β1 and β3 contained 'BH3-exon'. However, Bimβ1 and β3 proteins were not predicted to have the BH3 domain due to the frame shift that occurred by the insertion of the nucleotides transcribed from a novel exon (Fig. 1C,D). Thus, the α subgroup of Bim proteins had the BH3 domain and the β subgroup did not. Unlike the three isoforms reported previously, none of these novel isoforms had a hydrophobic region near the C-terminus. Bim_{EL} and Bim_L are reported to bind to the LC8 dynein light chain through the LC8-binding motif [13–15]. Among the novel isoforms, α1, α2, β1 and β2 had this motif.

3.2. Subcellular localizations of human Bim isoforms

To investigate the subcellular localizations of the Bim isoforms, expression plasmids encoding EGFP–Bim fusion proteins were constructed. To confirm the proper expression of each fusion protein, lysates obtained from transfected 293 cells were analyzed by immunoblotting using anti-GFP polyclonal antibody (Fig. 2). Proper-sized fusion proteins with comparable expression levels were detected in all lysates. This implies that there is no significant difference in stability among the Bim isoforms as a GFP-fused form. In HeLa cells, Bim_{EL} mainly localized in mitochondria as shown by the colocalization of green fluorescence with MitoTracker Red staining, although a significant level of green fluorescence was detected diffusely throughout the cell including the nu-

→

Fig. 1. Isolation of novel isoforms of Bim. A: Identification of multiple RT-PCR products of human *bim*. The coding region of human *bim* or *bid* cDNA was amplified by RT-PCR using polyA RNA from human fetal liver (lanes 1, 4), brain (lane 2) and lung (lane 3). The PCR products were subjected to agarose gel electrophoresis and photographed. B: A representative pattern of the *bim* expression profile. The RT-PCR products of human *bim* obtained using total RNA from the KB cell line (solid line) or testis (broken line) were analyzed with an Agilent 2100 bioanalyzer. The names of the isoforms and the lengths of the RT-PCR products in base pairs are indicated. C: Genomic organization of human *bim*. The human *bim* locus based on the Celera database is shown at the top. The lengths of variously shaded exons are indicated below in base pairs. The Bim isoforms are schematically depicted at the bottom with their lengths in number of amino acid residues. Arrows indicate the positions of the stop codons. D: Amino acid sequence alignment of human Bim isoforms. The dynein-binding motif, BH3 domain and hydrophobic tail are boxed. Amino acid residues are numbered to the left of each sequence. Dotted lines indicate gaps in the sequence for optimal alignment. The sequences frame-shifted from the previously reported isoforms are italicized. The C-termini of the isoforms are denoted by asterisks.

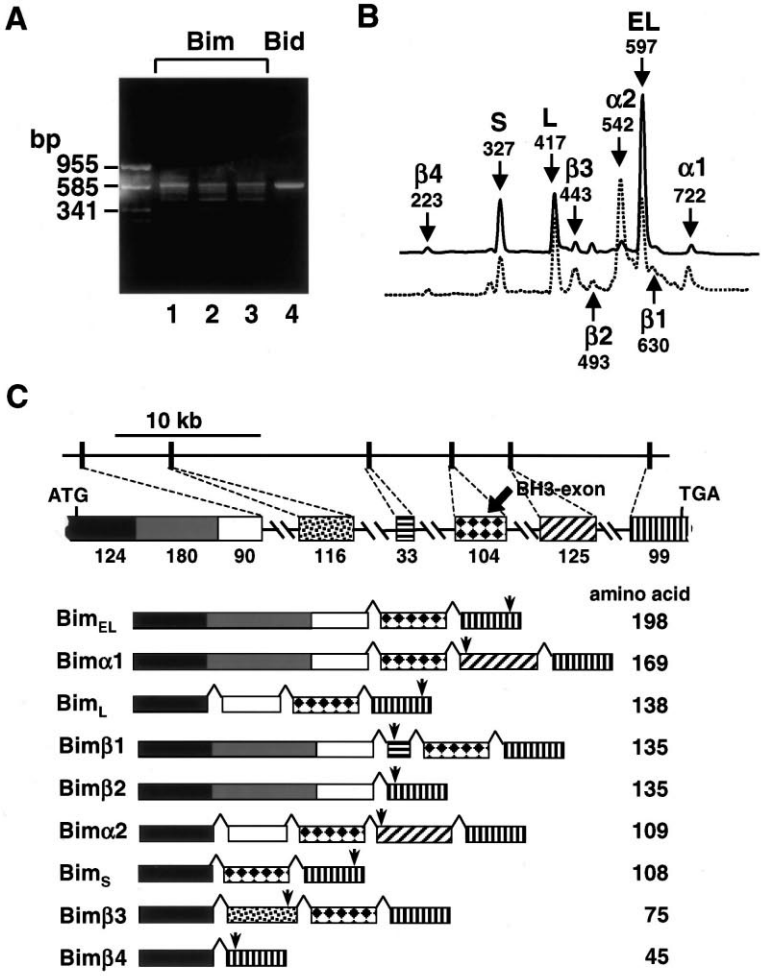

D

```
BimEL   1 MAKQPSDVSSECDREGRQLQPAERPPQLRPGAPTSLQTEPQGNPEGNHGGEGDSCPHGSP
BimL    1 MAKQPSDVSSECDREGRQLQPAERPPQLRPGAPTSLQTEPQ------------------
BimS    1 MAKQPSDVSSECDREGRQLQPAERPPQLRPGAPTSLQTEPQ------------------
Bimα1   1 MAKQPSDVSSECDREGRQLQPAERPPQLRPGAPTSLQTEPQGNPEGNHGGEGDSCPHGSP
Bimα2   1 MAKQPSDVSSECDREGRQLQPAERPPQLRPGAPTSLQTEPQ------------------
Bimβ1   1 MAKQPSDVSSECDREGRQLQPAERPPQLRPGAPTSLQTEPQGNPEGNHGGEGDSCPHGSP
Bimβ2   1 MAKQPSDVSSECDREGRQLQPAERPPQLRPGAPTSLQTEPQGNPEGNHGGEGDSCPHGSP
Bimβ3   1 MAKQPSDVSSECDREGRQLQPAERPPQLRPGAPTSLQTEPQVSLCHPGWSALVRSWLTAT
Bimβ4   1 MAKQPSDVSSECDREGRQLQPAERPPQLRPGAPTSLQTEPQGIFE*

                                                  Dynein-binding
BimEL  61 QGPLAPPASPGPFATRSPLFIFMRRSSLLSRSSSGYFSFDTDRSPAPMSCDKSTQTPSPP
BimL   42 ----------------------------------------DRSPAPMSCDKSTQTPSPP
BimS   42 ------------------------------------------------------------
Bimα1  61 QGPLAPPASPGPFATRSPLFIFMRRSSLLSRSSSGYFSFDTDRSPAPMSCDKSTQTPSPP
Bimα2  42 ----------------------------------------DRSPAPMSCDKSTQTPSPP
Bimβ1  61 QGPLAPPASPGPFATRSPLFIFMRRSSLLSRSSSGYFSFDTDRSPAPMSCDKSTQTPSPP
Bimβ2  61 QGPLAPPASPGPFATRSPLFIFMRRSSLLSRSSSGYFSFDTDRSPAPMSCDKSTQTPSPP
Bimβ3  61 SNSQVQAVLLPQPPK*

                                                BH3
BimEL 121 CQAFNHYLSAMASMRQAEPADMRPEIWIAQELRRIGDEFNAYYARRVFLNNYQAAEDHPR
BimL   61 CQAFNHYLSAMASMRQAEPADMRPEIWIAQELRRIGDEFNAYYARRVFLNNYQAAEDHPR
BimS   42 -----------ASMRQAEPADMRPEIWIAQELRRIGDEFNAYYARRVFLNNYQAAEDHPR
Bimα1 121 CQAFNHYLSAMASMRQAEPADMRPEIWIAQELRRIGDEFNAYYARRLEK*
Bimα2  61 CQAFNHYLSAMASMRQAEPADMRPEIWIAQELRRIGDEFNAYYARRLEK*
Bimβ1 121 CQAFNHYLSAMANWD*
Bimβ2 121 CQAFNHYLSAMGIFE*

          Hydrophobic region
BimEL 181 MVILRLLRYIVRLVWRMH*
BimL  121 MVILRLLRYIVRLVWRMH*
BimS   91 MVILRLLRYIVRLVWRMH*
```

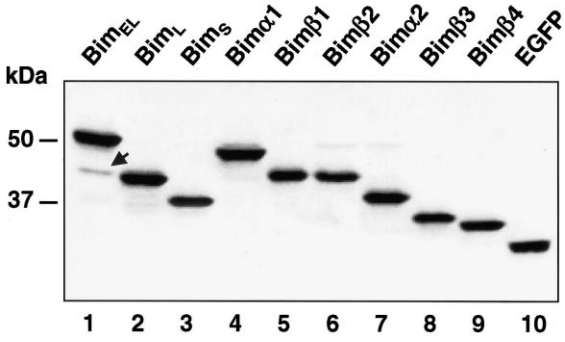

Fig. 2. Expression of EGFP–Bim fusion proteins. 293 cells were transfected with 2 μg of the EGFP–Bim constructs in the presence of 50 μM of zVAD-fmk. Cells were harvested at 24 h after transfection and subjected to SDS–PAGE followed by immunoblotting. The expressed proteins are indicated at the top of each panel. The faint band comigrating with EGFP–Bim_L, detected when transfected with pEGFP-Bim_{EL} (lane 1, arrow), is presumably due to the alternative splicing that occurred between the donor and acceptor sites within Bim_{EL} cDNA to generate Bim_L mRNA.

cleus (Fig. 3). MitoTracker Red staining was weaker in the cells expressing Bim_{EL}. Since the uptake of MitoTracker is dependent on the mitochondrial membrane potential ($\Delta\Psi_m$), BimEL was suggested to reduce $\Delta\Psi_m$, which is an early event of apoptosis. In this experiment, zVAD-fmk, a caspase inhibitor with a broad spectrum, was added to the culture just after the liposome treatment to prevent cell loss by apoptosis. Therefore, the reduction of $\Delta\Psi_m$ was not expected to be a consequence of caspase activation. In addition, in cells expressing Bim_{EL}, mitochondria were recruited to the perinuclear region. The subcellular localization of Bim_L and Bim_S was similar, but somewhat different from that of Bim_{EL}, as a significant fraction of cells showed a homogeneous distribution of these isoforms throughout the cell. Other cells showed a punctate pattern of distribution in the perinuclear region where they colocalized with mitochondria as shown in Bim_{EL}-expressing cells. Furthermore, mitochondrial staining with MitoTracker Red was almost absent in some cells expressing these isoforms indicating the complete disruption of $\Delta\Psi_m$. This is consistent with the observation that Bim_L and Bim_S are more potent inducers of cell death than Bim_{EL} [5]. The α subgroup of Bim isoforms showed a similar intracellular distribution to Bim_{EL}. In contrast, the β subgroup of Bim isoforms localized homogeneously both in the cytoplasm and in the nucleus. None of the cells showed a mitochondrial distribution or a reduction of MitoTracker staining, which indicates that these isoforms are deficient in cell death-inducing activities.

3.3. Proapoptotic functions of the novel isoforms

To investigate the Bim-mediated cell death more quantitatively, we measured luciferase activities of lysates obtained from 293 cells cotransfected with a GFP–Bim expression plasmid and a luciferase vector (Fig. 4A). In this assay, luciferase activities represent the relative cell numbers remaining in the

Table 1
The expression profiles of human *bim* isoforms in various tissues and cell lines

Tissue or cell line[a]	Total *bim* expression[b]	*bim* isoforms[c]								
		EL	L	S	α1	α2	β1	β2	β3	β4
Brain	1.6	36.7	13.2	18.3	5.8	9.5	5.9	2.1	5.3	3.4
Thymus	18.0	31.6	18.6	4.9	0.9	4.1	24.3	5.2	9.6	0.8
Heart	0.9	21.3	24.0	30.4	0.8	7.5	3.5	1.8	4.8	6.2
Trachea	17.2	37.6	13.6	7.3	1.1	5.7	21.0	3.4	9.0	1.3
Lung	29.9	42.5	24.7	4.7	0.7	5.3	8.2	1.8	11.2	0.9
Liver	4.8	15.3	23.5	29.0	0.3	5.9	3.9	1.3	17.7	3.4
Kidney	20.2	33.2	18.9	25.3	2.5	5.5	3.0	2.0	6.5	3.3
Spleen	14.2	36.0	25.9	18.7	1.7	4.1	1.9	4.6	3.3	4.1
Ovary	10.4	37.0	25.7	18.1	1.8	4.4	1.9	4.6	2.5	4.0
Testis	17.2	16.9	21.9	16.8	3.7	24.2	1.7	2.7	7.2	5.0
T98G	1.7	31.7	26.4	24.0	1.8	6.6	1.2	1.0	3.9	3.4
TGW	3.7	43.5	18.7	12.4	4.6	6.5	0.8	4.8	5.3	3.4
Y79	4.8	34.2	19.3	19.5	2.0	4.9	6.0	3.6	4.0	6.5
KB	1.2	37.4	20.4	24.4	1.4	4.7	1.8	2.3	3.2	4.4
MRC5	0.1	39.0	18.4	23.0	4.6	3.9	0.0	2.3	3.9	4.9
MCF7	20.2	41.6	18.5	19.2	0.8	5.3	4.4	1.1	7.7	1.4
HepG2	11.8	49.5	19.6	15.7	1.6	6.0	1.2	2.4	1.7	2.3
293	24.0	43.0	14.0	20.6	2.4	6.6	1.3	3.4	4.6	4.1
G401	2.8	34.7	18.7	22.3	4.8	7.6	0.8	2.6	5.0	3.5
HeLa	12.3	53.8	11.2	17.3	4.5	2.3	0.0	4.1	3.5	3.3
SCMC-ES-2	0.3	35.8	17.5	24.1	5.4	5.5	0.0	2.6	5.1	4.1
HOS	5.7	41.5	12.6	21.8	2.4	9.1	3.1	2.1	3.8	3.6
G292	2.4	42.1	19.2	14.8	3.1	5.4	1.5	4.5	2.6	6.8
MG63	0.3	30.1	20.0	25.4	2.5	4.7	0.0	3.5	4.3	9.5
Saos-2	6.7	49.4	16.0	15.6	2.1	5.7	2.9	3.2	2.6	2.5
697	11.1	29.5	21.6	25.1	4.7	8.4	6.1	0.8	2.9	0.9
Jurkat	3.8	36.4	30.1	11.2	1.6	8.0	6.6	2.1	1.5	2.6

[a]T98G, glioblastoma; TGW, neuroblastoma; Y79, retinoblastoma; KB, oropharyngeal epidermoid carcinoma; MRC-5, lung fibroblast; MCF7, breast cancer; HepG2, hepatoblastoma; 293, embryonic kidney; G401, Wilms' tumor; HeLa, cervical carcinoma; SCMC-ES-2, Ewing's sarcoma; HOS, osteosarcoma; G292, osteosarcoma; MG63, osteosarcoma; Saos-2, osteosarcoma; 697, pre-B cell leukemia; Jurkat, T cell leukemia.
[b]Human *bim* cDNA amplified by RT-PCR was analyzed with a 7700 ABI PRISM Sequence Detector System. The expression of *bim* normalized by *GAPDH* was shown as $\times 10^3$ copies/μg total RNA. The analysis was performed in triplicate.
[c]Human *bim* cDNA amplified by RT-PCR was analyzed with an Agilent 2100 bioanalyzer. The percentage of each isoform based on molarity is presented. The value is the mean calculated from at least two independent RT-PCRs.

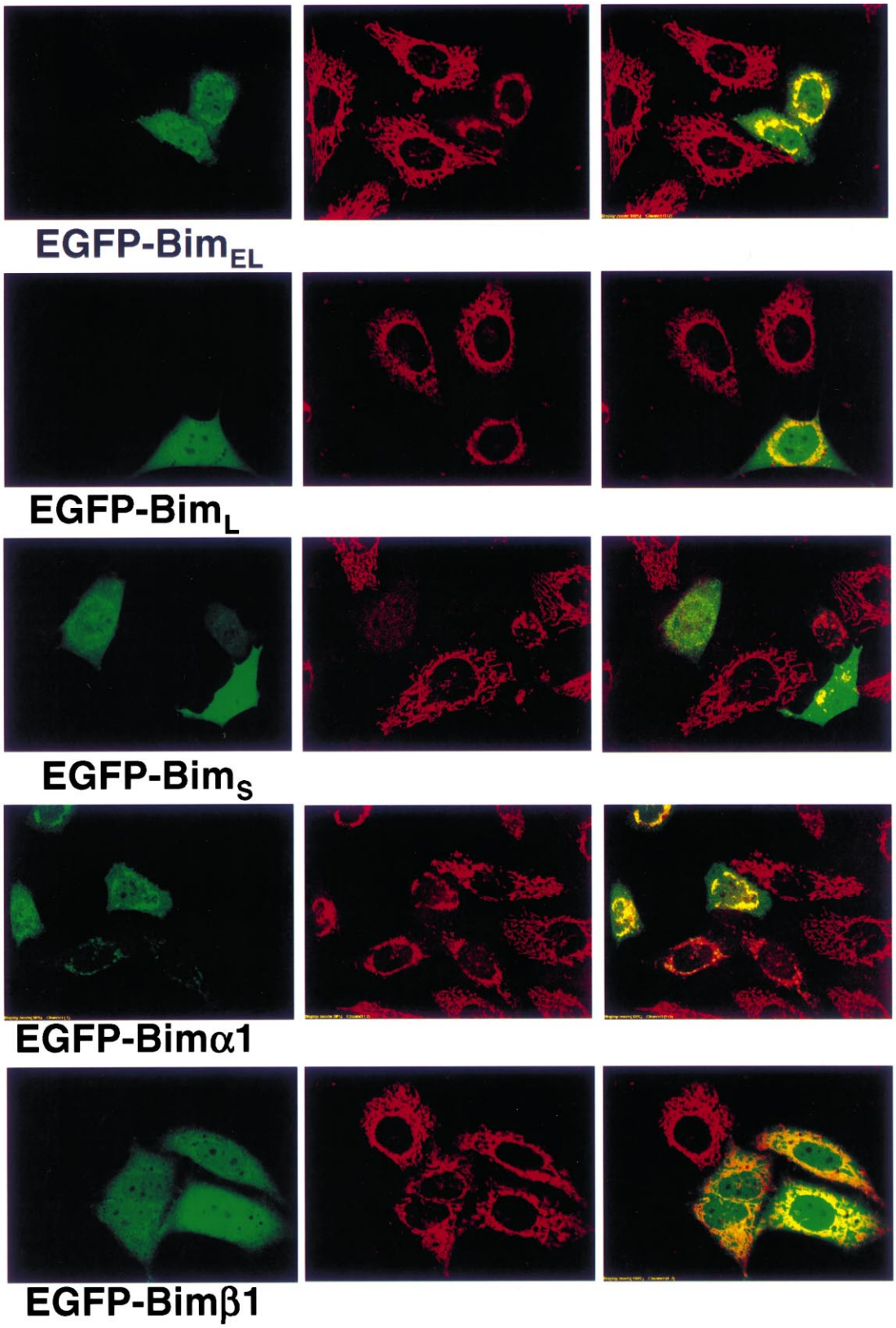

Fig. 3. Subcellular localization of Bim isoforms. 293 cells were transiently transfected with EGFP–Bim constructs as indicated below the images in the presence of 50 μM of zVAD-fmk. At 24 h after transfection, cells were stained with MitoTracker Red and fluorescence images were taken using a confocal microscope. Images in the middle row show MitoTracker Red fluorescence. Merged pictures are shown in the right row.

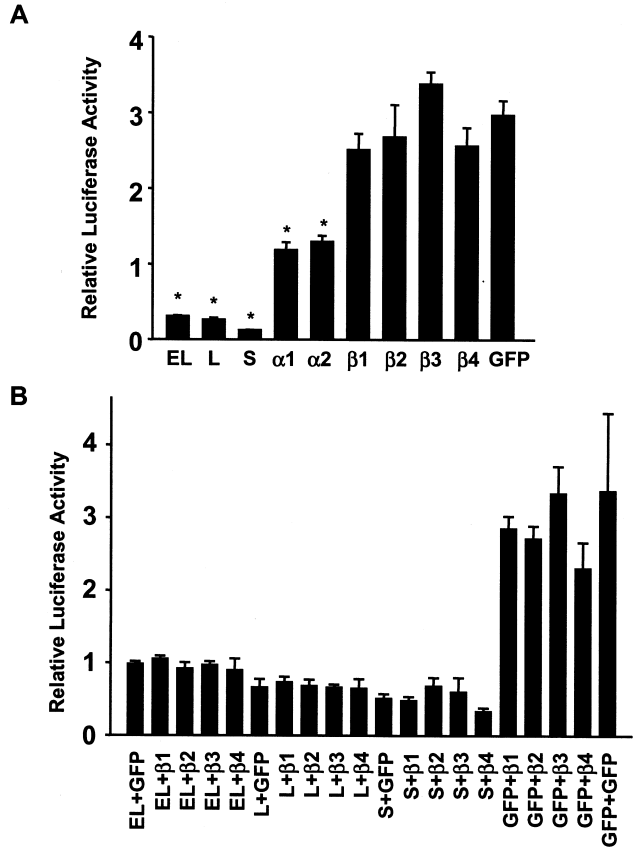

Fig. 4. Comparison of cell loss mediated by Bim isoforms. A: 293 cells were transfected with 1.5 μg of plasmid encoding the isoforms of Bim fused to EGFP in combination with 0.5 μg of luciferase plasmid. Cotransfection with plasmids encoding EGFP non-fusion protein and luciferase was included as a control (GFP). Cells were harvested 48 h after transfection and luciferase activities were measured. Data are presented as the mean ± standard error obtained from at least three independent experiments performed in triplicate. *$P < 0.01$ (vs. GFP by t test) B: 293 cells were transfected with various combinations of EGFP–Bim plasmids (0.9 μg) as indicated at the bottom along with luciferase plasmid (0.3 μg). Luciferase activity was measured as in A. A plasmid encoding EGFP non-fusion protein (GFP) was used to adjust the total amount of transfected DNA. Data are presented similarly as in A.

culture after the transfection. A marked decrease in luciferase activity was observed when cells were transfected with the classical three isoforms, i.e. the activity was 4–11% of that obtained when transfected with GFP non-fusion protein. As reported [5], Bim_S was the most potent inducer of cell death. A moderate, but significant decrease (41–44% of GFP non-fusion protein) was observed after the transfection with the α subgroup of isoforms. In contrast, the β subgroup of isoforms had a level of luciferase activity comparable to that of GFP non-fusion protein, indicating that these isoforms do not cause cell death.

Next, we tested the possibility that the β subgroup of isoforms which have no proapoptotic activity functions as a dominant negative inhibitor of the classical isoforms. In this experiment, 293 cells were cotransfected with various combinations of EGFP–Bim plasmids together with a luciferase vector. As shown in Fig. 4B, none of the β isoforms inhibited the cell death caused by the classical isoforms in a dominant negative manner.

3.4. Expression profiles of nine isoforms of bim in various tissues and cell lines

Since some isoforms are comprised of similar numbers of amino acid residues (i.e. L, β1 and β2 isoforms or S and α2 isoforms) and are phosphorylated under certain circumstances [8], it is expected to be impossible to analyze expression profiles by immunoblotting. Therefore, to determine the mRNA expression profiles of the *bim* isoforms, RT-PCR was performed using total RNA from a panel of tissues and cell lines, and profiles were analyzed with a 7700 ABI PRISM Sequence Detector System or an Agilent 2100 bioanalyzer. As shown in Table 1, the expression levels of total *bim* RNA were variable among human tissues. The brain, heart and liver showed very low levels of expression. Expression profiles of the *bim* isoforms were also highly variable among tissues. The classical isoforms were generally abundantly expressed. However, the percent expression of bim_S was much lower in the thymus, trachea and lung (4.7–7.3) than in other tissues (16.8–30.4). In addition, *bimα2* and *β3* were highly expressed in the testis and liver, respectively (24.2 and 17.7), whereas *β1* expression was higher in the thymus and trachea (24.3 and 21.0). In contrast, regardless of the total level of *bim* expression, the expression profiles in cancer or transformed cell lines were rather uniform with the three classical isoforms being the major forms. The percent expression of bim_{EL} ranged from 29.5 to 49.5, that of bim_L from 11.2 to 30.1 and that of bim_S from 11.2 to 25.4. All other isoforms were expressed at less than 10%. As far as we examined, cell lines did not reflect the expression profiles of their parental normal tissues.

4. Discussion

To our knowledge, among BH3-only Bcl-2 family members, Bim and PUMA (p53 upregulated modulator of apoptosis) are known to have isoforms due to alternative splicing [5,16]. In this study, we have identified and characterized six novel isoforms of Bim. Our results are summarized in Table 2.

Table 2
Summary of structure–distribution and structure–function relationship

Bim isoform	Bim_{EL}	Bim_L	Bim_S	Bimα1	Bimα2	Bimβ1	Bimβ2	Bimβ3	Bimβ4
BH3	+	+	+	+	+	−	−	−	−
Hydrophobic region	+	+	+	−	−	−	−	−	−
Dynein-binding motif	+	+	−	+	+	+	+	−	−
Mitochondrial distribution[a]	++	+	+	++	±	−	−	−	−
Reduced $\Delta\Psi_m^b$	+	++	++	+	+	−	−	−	−
Cell death[c]	++	++	++	+	+	−	−	−	−

[a,b]++: more than 90% of the transfected cells fall into this category, +: 20–90% of the transfected cells fall into this category, ±: less than 20% of the transfected cells fall into this category, −: none of the transfected cells fall into this category.
[c]Based on Fig. 4A.

Among Bim isoforms, only those that have the BH3 domain showed proapoptotic activity. However, cell death-inducing activities of the α subgroup of isoforms were much weaker than those of the classical isoforms, suggesting that the BH3 domain is necessary but not sufficient for the induction of cell death. It is likely that the C-terminal hydrophobic region is required for the full activity of Bim. In contrast, the BH3 domain was sufficient for Bim to localize in mitochondria, as we found the α subgroup successfully distributed in mitochondria. Since the BH3 domain is responsible for the binding to anti-apoptotic Bcl-2 family members such as Bcl-x_L, these findings imply that this binding but not membrane anchoring plays an important role in the mitochondrial localization. The failure of the β subgroup isoforms to act as a dominant negative molecule of the classical isoforms suggests that β subgroup does not inhibit the classical forms from binding to anti-apoptotic Bcl-2 family proteins.

Bim_{EL} and Bim_L are reported to interact with the LC8 cytoplasmic dynein light chain in healthy cells and, during induction of apoptosis, are released together with LC8 from the dynein motor complex and translocate to mitochondria [13]. The Bim–LC8 interaction is mediated by the LC8-binding motif, KXTQT [13–15]. Although a typical punctate or vesicular distribution, which is indicative of the cytoplasmic dynein distribution in interphase cells [17–19], was not demonstrated in the cells transfected with the isoforms containing the LC8-binding motif, some of the molecules distributed in the cytosol may bind to LC8. Interestingly, the BH3-containing isoforms partially colocalized with mitochondria simply by overexpression. Overexpression of the proapoptotic Bim isoforms or liposome-mediated transfection itself may be sufficient to trigger apoptotic signaling which leads to the dissociation of the Bim protein from the dynein complex and the translocation to mitochondria.

bim RNA was widely expressed in human tissues as reported earlier [20]. A low expression in the brain, heart and liver may reflect a low turnover rate of these tissues due to a suppressed apoptosis. Interestingly, unlike tumor or transformed cells that showed rather uniform profiles of isoform expression, highly variable profiles were observed in normal tissues, suggesting a tissue-specific transcriptional regulation of the *bim* isoforms. Based on our findings that some isoforms of Bim have proapoptotic activity to some degree and others do not, the regulation of the expression of *bim* isoforms may fine-tune the proapoptotic activity of Bim, resulting in either an amplification or inhibition of the apoptotic response of tissues or cells.

Acknowledgements: We thank Yuko Ohtsuka and Atsuko Asaka for technical assistance and Kayoko Saito for preparing the manuscript. This study was supported in part by grants for Brain Research and for Genome Research from the Ministry of Health, Labor and Welfare, a Grant-in-Aid for Scientific Research, and a Grant for Organized Research Combination System from the Ministry of Education, Culture, Sports, Science and Technology.

References

[1] Thompson, C.B. (1995) Science 267, 1456–1462.
[2] Roy, S. and Nicholson, D.W. (2000) J. Exp. Med. 192, F21–F25.
[3] Gross, A., McDonnell, J.M. and Korsmeyer, S.J. (1999) Genes Dev. 13, 1899–1911.
[4] Huang, D.C. and Strasser, A. (2000) Cell 103, 839–842.
[5] O'Connor, L., Strasser, A., O'Reilly, L.A., Hausmann, G., Adams, J.M., Cory, S. and Huang, D.C. (1998) EMBO J. 17, 384–395.
[6] Bouillet, P., Metcalf, D., Huang, D.C., Tarlinton, D.M., Kay, T.W., Kontgen, F., Adams, J.M. and Strasser, A. (1999) Science 286, 1735–1738.
[7] Dijkers, P.F., Medema, R.H., Lammers, J.W., Koenderman, L. and Coffer, P.J. (2000) Curr. Biol. 10, 1201–1204.
[8] Shinjyo, T., Kuribara, R., Inukai, T., Hosoi, H., Kinoshita, T., Miyajima, A., Houghton, P.J., Look, A.T., Ozawa, K. and Inaba, T. (2001) Mol. Cell. Biol. 21, 854–864.
[9] Putcha, G.V., Moulder, K.L., Golden, J.P., Bouillet, P., Adams, J.A., Strasser, A. and Johnson, E.M. (2001) Neuron 29, 615–628.
[10] Miyashita, T., Okamura-Oho, Y., Mito, Y., Nagafuchi, S. and Yamada, M. (1997) J. Biol. Chem. 272, 29238–29242.
[11] Shikama, Y., U, M., Miyashita, T. and Yamada, M. (2001) Exp. Cell Res. 264, 315–325.
[12] Pawlowski, V., Revillion, F., Hornez, L. and Peyrat, J.P. (2000) Cancer Detect. Prev. 24, 212–223.
[13] Puthalakath, H., Huang, D.C., O'Reilly, L.A., King, S.M. and Strasser, A. (1999) Mol. Cell 3, 287–296.
[14] Rodríguez-Crespo, I., Yélamos, B., Roncal, F., Albar, J.P., Ortiz, d.M.P. and Gavilanes, F. (2001) FEBS Lett. 503, 135–141.
[15] Lo, K.W., Naisbitt, S., Fan, J.S., Sheng, M. and Zhang, M. (2001) J. Biol. Chem. 276, 14059–14066.
[16] Nakano, K. and Vousden, K.H. (2001) Mol. Cell 7, 683–694.
[17] Pfarr, C.M., Coue, M., Grissom, P.M., Hays, T.S., Porter, M.E. and McIntosh, J.R. (1990) Nature 345, 263–265.
[18] Steuer, E.R., Wordeman, L., Schroer, T.A. and Sheetz, M.P. (1990) Nature 345, 266–268.
[19] Tai, A.W., Chuang, J.Z. and Sung, C.H. (1998) J. Biol. Chem. 273, 19639–19649.
[20] O'Reilly, L.A., Cullen, L., Visvader, J., Lindeman, G.J., Print, C., Bath, M.L., Huang, D.C. and Strasser, A. (2000) Am. J. Pathol. 157, 449–461.